Superconductivity and multiple pressure-induced phases in $BaPt_2As_2$

C. Y. Guo,[1] W. B. Jiang,[1] M. Smidman,[1] F. Han,[2,3,4] C. D. Malliakas,[2,5] B. Shen,[1] Y. F. Wang,[1] Y. Chen,[1] X. Lu,[1,6] M. G. Kanatzidis,[2,5] and H. Q. Yuan[1,6,*]

[1]*Center for Correlated Matter and Department of Physics, Zhejiang University, Hangzhou 310058, China*
[2]*Materials Science Division, Argonne National Laboratory, Argonne, Illinois 60439, USA*
[3]*HPSynC, Geophysical Laboratory, Carnegie Institution of Washington, Argonne, Illinois 60439, USA*
[4]*Center for High Pressure Science and Technology Advanced Research, Beijing 100094, People's Republic of China*
[5]*Department of Chemistry, Northwestern University, Evanston, Illinois 60208, USA*
[6]*Collaborative Innovation Center of Advanced Microstructures, Nanjing 210093, China*

(Received 14 July 2016; revised manuscript received 24 October 2016; published 16 November 2016)

The recently discovered $BaPt_2As_2$ shows a structural distortion at around 275 K, followed by the emergence of superconductivity at lower temperatures. Here we identify the presence of charge-density-wave order at room temperature and ambient pressure using single-crystal x-ray diffraction, with both a superlattice and an incommensurate modulation, where there is a change of the superlattice structure below $\simeq$275 K. Upon applying pressure, $BaPt_2As_2$ shows a rich temperature-pressure phase diagram with multiple pressure-induced transitions at high temperatures, the emergence or disappearance of which are correlated with sudden changes in the superconducting transition temperature T_c. These findings demonstrate that $BaPt_2As_2$ is a promising system for studying competing interactions and the relationship between high-temperature electronic instabilities and superconductivity.

DOI: 10.1103/PhysRevB.94.184506

I. INTRODUCTION

The presence of competing interactions and multiple electronic instabilities often leads to emergent phenomena and new phases. In particular, the complex relationship between superconductivity and magnetic or charge order has attracted considerable interest. In many of the high-temperature iron-pnictide superconductors, the superconductivity occurs in the vicinity of spin-density-wave (SDW) order [1,2]. Meanwhile, upon applying pressure to the heavy-fermion superconductor $CeCu_2Si_2$ [3], evidence was found of superconductivity being in close proximity to multiple instabilities, with one superconducting dome in the vicinity of magnetic order and another near a possible valence instability [4–6]. The interplay between charge-density-wave (CDW) order and superconductivity has also been of particular interest recently [7,8], mainly due to the coexistence of these competing phases in some systems, with a similar phase diagram to systems with SDW and superconductivity [9], as well as the observation of CDW in high-temperature cuprate superconductors. In the cuprates, the role of CDW order in the formation of superconductivity remains a central and open issue [10–15], but the microscopic relationship is still unresolved.

Structural distortions have also been found to occur in various iron-based superconductors [16]. For instance, upon lowering the temperature of electron-doped $BaFe_2As_2$, the symmetry of the crystal lattice is reduced from the fourfold symmetry of the $ThCr_2Si_2$ structure to a twofold symmetric orthorhombic structure, while SDW ordering onsets at lower temperatures [17,18]. There is an increasing body of evidence that this distortion does not arise due to phonons [19], but is from an electronic instability, the nematic order, which may be driven by either spin or orbital fluctuations [20]. The suppression of both nematicity and SDW ordering in the region of the superconducting dome again indicates the importance of understanding the relationship between the various ordered phases and the underlying interactions. On the other hand, there also exist some non-iron-based 122 pnictide superconductors RT_2Pn_2 (R = Ba or Sr, T denotes transition metal, and Pn denotes pnictogen) that undergo structural distortions upon cooling [21–23]. A comparison with the iron-based materials may provide crucial insights into the roles of various interactions and the resulting collective phenomena.

Unlike the 122 iron-pnictide superconductors, which crystallize in the $ThCr_2Si_2$ structure ($I4/mmm$), $SrPt_2As_2$ forms in the $CaBe_2Ge_2$-type structure ($P4/nmm$) at high temperatures. Both are layered tetragonal structures, but they have different stacking of the layers of transition metal and As atoms along the c axis. A further difference from the iron pnictides is that in the Pt-based materials, spin fluctuations are not generally expected to play a significant role. Below $T_{CDW} = 470$ K, the crystal structure of $SrPt_2As_2$ undergoes an orthorhombic distortion and CDW ordering [24–27], with a superconducting transition at a lower temperature of 5.2 K [22]. Similarly, in the newly discovered $BaPt_2As_2$ with a resistive transition at $T_c = 1.67$ K [28], a first-order phase transition appears at about 275 K, at which a structural phase transition from the tetragonal $CaBe_2Ge_2$-type structure to an orthorhombic structure was found using powder x-ray diffraction (XRD) [28]. In this article, we demonstrate using single-crystal XRD measurements that a CDW state already exists at room temperature in $BaPt_2As_2$, and the structural transition at $T_1 \simeq 275$ K corresponds to a change in the CDW superlattice. To study the relationship between superconductivity and the CDW state, we performed resistivity measurements under pressure, which reveal a rich temperature-pressure phase diagram with multiple pressure-induced transitions, the emergence of which are correlated with sudden changes in T_c.

*hqyuan@zju.edu.cn

II. EXPERIMENTAL METHODS

Single crystals of $BaPt_2As_2$ were synthesized using a self-flux method described in Ref. [28]. Resistivity measurements under pressure were carried out using a piston-cylinder-type pressure cell up to 27 kbar, and Daphne 7373 was used as the pressure-transmitting medium to ensure hydrostaticity. The applied pressure was determined by the shift in T_c of a high-quality Pb single crystal. Measurements were performed using a Physical Property Measurement System (Quantum Design PPMS-14T) in the temperature range of 2–300 K, while measurements from 0.3 to 5 K were performed using a ^{3}He refrigerator. Single-crystal XRD from room temperature to 100 K was carried out on a STOE IPDS II diffractometer at the Argonne National Laboratory, using an Mo source ($\lambda = 0.710\,73$ Å). Reciprocal space reconstruction of the single-crystal XRD data was performed with the software X-AREA.

III. RESULTS

A. Single-crystal x-ray diffraction

A simulation of the diffraction peaks in the $(hk0)$ plane for the tetragonal $CaBe_2Ge_2$-type structure ($P4/nmm$) is shown in Fig. 1(a), while the reciprocal space reconstruction of single-crystal XRD data at 300 and 100 K is shown in Figs. 1(b) and 1(c), respectively. Reflections are labeled with the Miller indices of the $CaBe_2Ge_2$-type structure ($P4/nmm$).

In the previous powder XRD measurements [28], we reported a structural phase transition at 275 K from a tetragonal $CaBe_2Ge_2$-type structure to an orthorhombic one. Based on the current single-crystal XRD results, it should be noted that neither the reflections at 300 K nor those at 100 K could be satisfactorily indexed with a perfect $CaBe_2Ge_2$-type crystal structure. From comparing the experimental data at both 300 and 100 K with the simulated reflections, we observe a number of additional peaks arising from complex CDW modulations. If we index the single-crystal XRD data by introducing an orthorhombic distortion, the lattice parameters at 300 K are $a = 4.5608(10)$ Å, $b = 4.5643(12)$ Å, and $c = 10.0420(20)$ Å, while at 100 K they are $a = 4.5489(9)$ Å, $b = 4.5700(11)$ Å, and $c = 10.0192(22)$ Å. These results indicate that even at room temperature, the CDW modulations induce a small difference in a and b, which becomes larger below 280 K. Subsequent analysis of the data at 300 K reveals peaks corresponding to $2 \times 2 \times 2$ superlattice structure, where the unit cell is doubled in all directions, along with an incommensurate modulation $\mathbf{q_1} = (0.1,0.3,0)$. Reflections that are forbidden for the $CaBe_2Ge_2$-type structure, such as $(1,0,0)$ and $(0,1,0)$, and the half-fractional peaks such as $(-1/2, -1/2,0)$ arise from the $2 \times 2 \times 2$ superlattice structure, while the peaks at the position of $(0.1,0.3,0)$ around the superlattice peaks arise from the incommensurate modulation. A comparison of the data from 300 to 285 K shows no change in the structure of $BaPt_2As_2$. From 280 to 100 K, $BaPt_2As_2$ enters a new phase in which the symmetry further lowers to a $6 \times 6 \times 2$ superlattice structure while the incommensurate modulation $\mathbf{q_1}$ remains the same, as indicated by the appearance of new fractional peaks such as $(2/3,0,0)$ and $(0,2/3,0)$. Therefore, these results demonstrate that the CDW state is already present at room temperature, but there is a change in CDW structure below 280 K, along with an increased orthorhombic distortion.

B. Resistivity under pressure

The temperature-pressure phase diagram of $BaPt_2As_2$ was determined by measuring the resistivity under pressure. As shown in Fig. 2(a), at $p = 3$ kbar there is a sudden increase of the resistivity upon cooling at about $T_1 \simeq 250$ K, which is similar to the previously reported results at ambient pressure [28], and it corresponds to a change of the CDW structure. With increasing pressure, the temperature of this transition decreases before abruptly disappearing above $p_1 \simeq 7$ kbar. After T_1 disappears, a new transition labeled T_2 is observed, where there is only a small anomaly in the resistivity and little change with increasing pressure. For pressures greater than $p_2 \simeq 17$ kbar, T_2 disappears and two new transitions

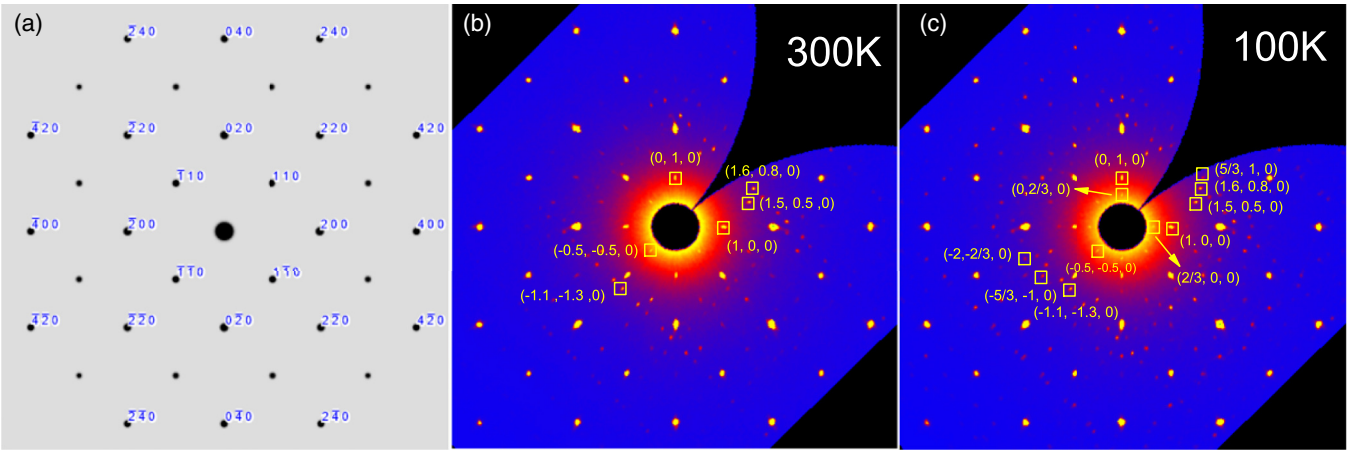

FIG. 1. Reciprocal space reconstruction of single-crystal XRD. (a) Simulated diffraction peaks in the $(hk0)$ plane of reciprocal space for the $CaBe_2Ge_2$-type structure. Reciprocal space reconstruction of the single-crystal XRD data collected at (b) 300 K and (c) 100 K. At 300 K, other than the simulated peaks of the $CaBe_2Ge_2$-type structure, there are satellite peaks which can be indexed with a $2 \times 2 \times 2$ superlattice and an incommensurate modulation with a propagation vector $\mathbf{q_1} = (0.1,0.3,0)$. At 100 K, additional satellite peaks corresponding to a $6 \times 6 \times 2$ superlattice are observed.

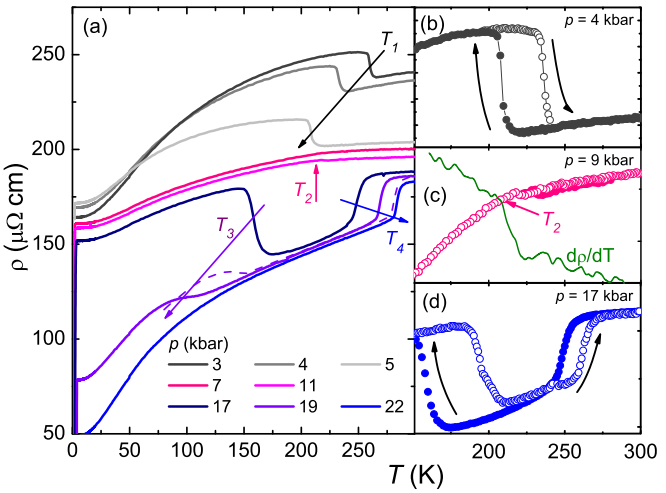

FIG. 2. (a) Temperature dependence of the resistivity of $BaPt_2As_2$ at various pressures. The different high-temperature transitions are denoted by T_1, T_2, T_3, and T_4. The resistivity upon warming and cooling is shown in the vicinity of (b) T_1 at 4 kbar, (c) T_2 at 9 kbar, and (d) T_3 and T_4 at 17 kbar. In (c) the derivative $d\rho/dT$ is also shown by the solid line, which shows a clear change at T_2.

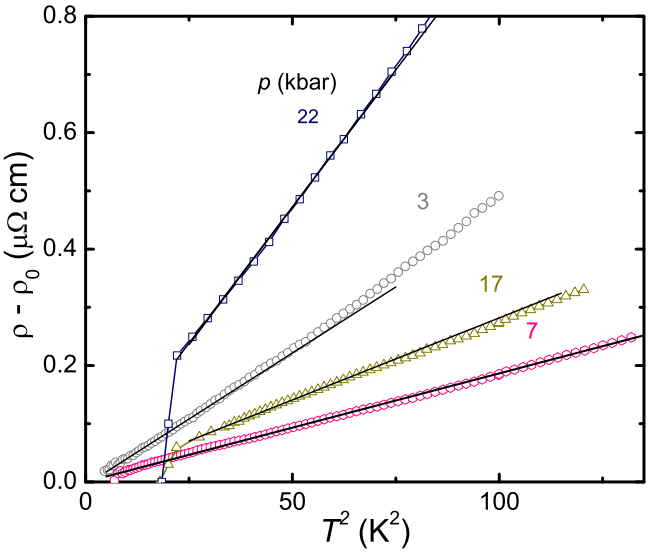

FIG. 4. Resistivity as a function of T^2 at several pressures with the residual values ρ_0 subtracted. The solid lines show fits to a $\sim T^2$ dependence in the normal state.

emerge at T_3 and T_4, with the former corresponding to an increase of the resistivity upon cooling, while the latter shows a sudden decrease. These transitions have a different pressure dependence, with the lower transition T_3 being rapidly suppressed with increasing pressure while T_4 increases with pressure. Note that apart from T_2, all the transitions display pronounced hysteresis, as shown in Figs. 2(b)–2(d), indicating a first-order nature. It can also be seen that there is an increase in resistivity at T_1 and T_3 while it drops at T_4.

Figure 3(a) displays the resistivity under pressure at low temperatures in the vicinity of the superconducting transitions. At ambient pressure, T_c is about 1.6 K, determined from where the resistivity reaches 50% of the normal state value $\rho_0 \simeq 174\,\mu\Omega$ cm, similar to that previously reported [28]. With

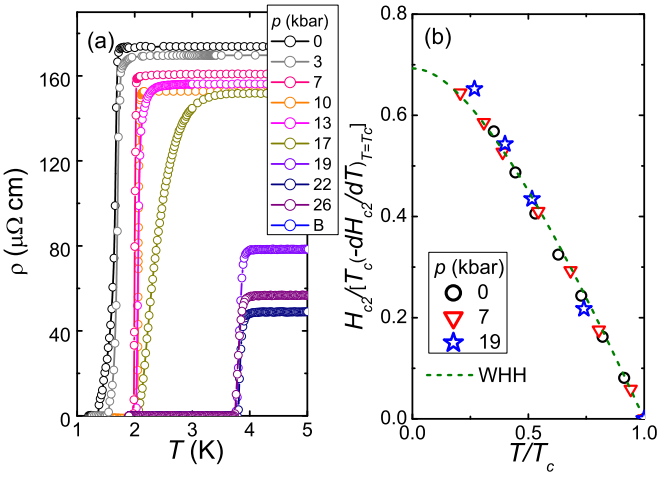

FIG. 3. (a) Resistivity of $BaPt_2As_2$ at various pressures, near the superconducting transition. (b) The upper critical field (H_{c2}) of $BaPt_2As_2$ as a function of T/T_c at various pressures, normalized by the product of T_c and the slope of H_{c2} near T_c.

increasing pressure, the superconducting transition sharpens and T_c undergoes a moderate enhancement at around 7 kbar, which is close to p_1, to around 2 K, along with a small decrease of ρ_0. Further increasing the pressure up to 13 kbar results in little change of T_c. However, upon applying pressures greater than 13 kbar, there is another jump in T_c that is larger in size, reaching a near constant value above 17 kbar. The superconducting transition at 17 kbar is significantly broader than that at both lower and higher pressures, which may be due to a pressure inhomogeneity, leading to the coexistence of both superconducting phases. The newly emerged superconducting phase has the highest $T_c \simeq 3.8$ K, the lowest residual resistivity in the normal state, and T_c changes little with pressure up to 26 kbar. The upper critical field $H_{c2}(T)$ at different pressures is shown in Fig. 3(b). The values of H_{c2} were measured in three regions of the temperature-pressure phase diagram (0, 7, and 19 kbar), and they were normalized by the product of T_c and the derivative of H_{c2} near T_c. When the normalized H_{c2} is plotted as a function of T/T_c, all the data fall on one curve, in good agreement with the orbital limited values of H_{c2} calculated using the Werthamer-Helfand-Hohenberg (WHH) model shown by the dashed line [29]. This suggests that there is no change of the superconducting pairing state under pressure, and that orbital limiting rather than Pauli limiting is the dominant pair breaking mechanism. Meanwhile, as displayed in Fig. 4, the low-temperature normal state resistivity could be well fitted with Fermi liquid behavior, $\rho(T) = \rho_0 + AT^2$.

Figure 5(a) displays the temperature-pressure phase diagram obtained from resistivity measurements. Two abrupt enhancements of T_c occur under pressure, both of which clearly coincide with changes in the high-temperature phase transitions. At $p_1 \simeq 7$ kbar, the CDW transition at T_1 disappears and a new transition T_2 is observed. This change is accompanied by an enhancement of T_c. Upon further increasing the applied pressure, there is little change of T_2 up to $p_2 \simeq 17$ kbar, where the transition at T_2 is no longer observed

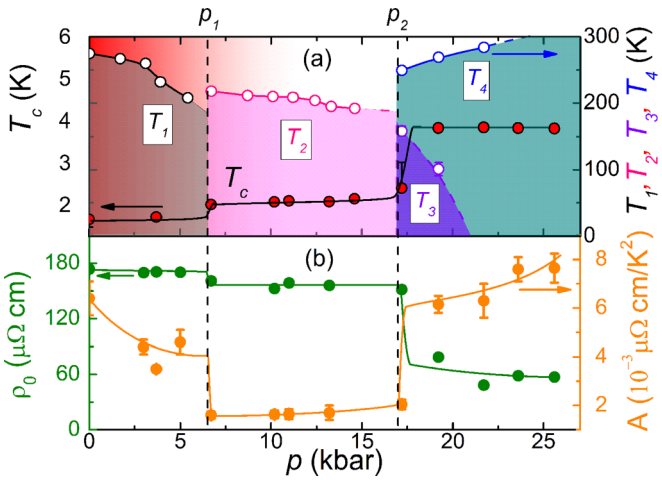

FIG. 5. (a) Temperature-pressure phase diagram of $BaPt_2As_2$ showing both the high-temperature and superconducting transitions. (b) Pressure dependence of the residual resistivity ρ_0 and A coefficient.

and two new phase transitions emerge. The transition at T_3 decreases with increasing pressure before being suppressed at less than 22 kbar, while T_4 increases with pressure, reaching 290 K at 24 kbar. The appearance of these transitions is accompanied by another pronounced enhancement of T_c by almost a factor of 2. The critical pressure for the emergence of T_3 and T_4 is slightly lower than that corresponding to the jump in T_c. This may be due to the variation in the pressure transmitted by the Daphne 7373 medium with temperature, which can cause a pressure decrease of around 1–2 kbar between 300 K and low temperatures [30]. Furthermore, the results from fitting the resistivity in the normal state are shown in Fig. 5(b). Each steplike increase of T_c coincides with a drop in ρ_0, with a small decrease at the disappearance of T_1 and a larger drop at the emergence of T_3 and T_4. Meanwhile, the resistivity coefficient A undergoes a sharp drop at p_1 followed by a sudden increase at p_2. Furthermore, neither ρ_0 nor A displays any noticeable anomaly upon the disappearance of the transition at T_3.

IV. DISCUSSION AND SUMMARY

The above results demonstrate an intricate relationship between the superconductivity and the high-temperature transitions in $BaPt_2As_2$. The nature of the transitions at T_2, T_3, and T_4 is yet to be uncovered. In comparison, $SrPt_2As_2$ undergoes a structural phase transition below $T_{CDW} = 470$ K, from a tetragonal to orthorhombic structure [25], with two incommensurate CDW modulations emerging [24,26]. However, in $BaPt_2As_2$ at ambient pressure the orthorhombic distortion and CDW modulation already exist above T_1, and this transition corresponds to a change of the periodicity of the superlattice. Furthermore, there is a sudden increase in the resistivity at T_1 as in the case of the structural transition in $SrNi_2P_2$ [31], whereas there is a drop in the resistivity at T_{CDW} in $SrPt_2As_2$. However, the behavior of $BaPt_2As_2$ above 22 kbar more strongly resembles that of $SrPt_2As_2$, since we observe a drop in the resistivity at T_4 and there is a comparable value of T_c.

If then the transition under pressure at T_4 is similar to that of $SrPt_2As_2$ at ambient pressure, the differences in the CDW modulation and high-temperature crystal structures may explain the different behavior of the resistivity seen at T_1 and T_4. This suggests the possibility that the CDW state below T_1 disappears at p_1, above which only a weak anomaly at T_2 is observed. Furthermore, it is not clear whether the CDW state observed at ambient pressure and room temperature persists upon the application of pressure, and it may be that the transition at T_2 lies beneath a CDW transition at higher temperatures. At p_2, a different CDW state may emerge. However, while CDW states generally compete with superconductivity, in this instance the emergence of the transition at T_4 leads to a significant enhancement of T_c, rather than a decrease. The dramatic change in both ρ_0 and the A coefficient at p_2 suggests that this may correspond to a sudden change in the electronic structure and Fermi surface topology. Such changes may lead to an enhanced density of states, which in turn may cause the significant increase of T_c and A.

The transition at T_3, which appears under T_4 up to around 19 kbar, may then correspond to a further lowering of the crystal symmetry or a change in the modulation vector $\mathbf{q}$ of the CDW state. A change of $\mathbf{q}$ can lead to different behavior of the resistivity since this changes the reconstructed Fermi surface, with the CDW gap opening across different regions. However, for these scenarios it would be unusual that there is little change in T_c upon the disappearance of T_3. As previously discussed, at ambient pressure there is a structural distortion at T_1 corresponding to a significantly increased orthorhombicity. Since both T_3 and T_4 have a similar first-order nature, whether these transitions correspond to changes in either the crystal symmetry or structural parameters needs to be checked with XRD measurements under pressure. All these results suggest the presence of both structural and electronic instabilities in the temperature-pressure phase diagram. In light of the recent evidence that the nematic order in the iron-pnictide-based superconductors is driven by electronic rather than structural instabilities [20], it will be of interest to determine whether any of the transitions or structural changes in $BaPt_2As_2$ also have an electronic origin. The relationship between the high-temperature transitions and the superconductivity also needs to be further investigated and compared to both the cuprate- and iron-based materials, but the significantly lower values of T_c may be a result of the lack of a spin fluctuation mediated pairing mechanism.

In conclusion, using single-crystal XRD measurements, we have identified that a CDW state exists in $BaPt_2As_2$ in ambient conditions, and that the transition at $T_1 = 275$ K corresponds to a change of the superlattice structure. The application of pressure results in a rich phase diagram. Pressure suppresses the CDW transition at T_1 until it disappears at around $p_1 = 7$ kbar, which leads to an enhancement of T_c. Upon further increasing the pressure, new high-temperature transitions are observed in the resistivity, which are correlated with an additional increase of T_c. Since these results indicate the presence of multiple instabilities at high temperatures, $BaPt_2As_2$ may provide a platform for studying the competition between different interactions and their interplay with superconductivity. Further experiments such as NMR and XRD under pressure, as well as theoretical calculations, are needed

to characterize the origin of these transitions and elucidate the mechanisms that lead to these exotic behaviors.

ACKNOWLEDGMENTS

We thank C. Cao for interesting discussions. The work at Zhejiang University was supported by the National Natural Science Foundation of China (Grants No. 11474251 and No. 11374257), the National Key R&D Program of China (Grant No. 2016YFA0300202) and the Science Challenge Program of China. The work at Argonne was supported by the Office of Science, Office of Basic Energy Sciences, Division of Materials Sciences, US Department of Energy, under Contract No. DE-AC02-06CH11357 (BES-DMSE).

[1] J. Paglione and R. L. Greene, High-temperature superconductivity in iron-based materials, Nat. Phys. **6**, 645 (2010).

[2] X. H. Chen, P. C. Dai, D. L. Feng, T. Xiang, and F.-C. Zhang, Iron-based high transition temperature superconductors, Natl. Sci. Rev. **1**, 371 (2014).

[3] F. Steglich, J. Aarts, C. D. Bredl, W. Lieke, D. Meschede, W. Franz, and H. Schäfer, Superconductivity in the Presence of Strong Pauli Paramagnetism: $CeCu_2Si_2$, Phys. Rev. Lett. **43**, 1892 (1979).

[4] P. Gegenwart, C. Langhammer, C. Geibel, R. Helfrich, M. Lang, G. Sparn, F. Steglich, R. Horn, L. Donnevert, A. Link, and W. Assmus, Breakup of Heavy Fermions on the Brink of Phase A in $CeCu_2Si_2$, Phys. Rev. Lett. **81**, 1501 (1998).

[5] H. Q. Yuan, F. M. Grosche, M. Deppe, C. Geibel, G. Sparn, and F. Steglich, Observation of two distinct superconducting phases in $CeCu_2Si_2$, Science **302**, 2104 (2003).

[6] A. T. Holmes, D. Jaccard, and K. Miyake, Signatures of valence fluctuations in $CeCu_2Si_2$ under high pressure, Phys. Rev. B **69**, 024508 (2004).

[7] For a review, see A. M. Gabovich, A. I. Voitenko, and M. Ausloos, Charge- and spin-density waves in existing superconductors: Competition between Cooper pairing and Peierls or excitonic instabilities, Phys. Rep. **367**, 583 (2002).

[8] M. Hoesch, X. Cui, K. Shimada, C. Battaglia, S. Fujimori, and H. Berger, Splitting in the Fermi surface of $ZrTe_3$: A surface charge density wave system, Phys. Rev. B **80**, 075423 (2009).

[9] E. Morosan, H. W. Zandbergen, B. S. Dennis, J. W. G. Bos, Y. Onose, T. Klimczuk, A. P. Ramirez, N. P. Ong, and R. J. Cava, Superconductivity in Cu_xTiSe_2, Nat. Phys. **2**, 544 (2006).

[10] J. M. Tranquada, B. J. Sternlieb, J. D. Axe, Y. Nakamura, and S. Uchida, Evidence for stripe correlations of spins and holes in copper oxide superconductors, Nature (London) **375**, 561 (1995).

[11] T. Wu, H. Mayaffre, S. Krämer, M. Horvatić, C. Berthier, W. N. Hardy, R. Liang, D. A. Bonn, and M. Julien, Magnetic-field-induced charge-stripe order in the high-temperature superconductor $YBa_2Cu_3O_y$, Nature (London) **477**, 191 (2011).

[12] G. Ghiringhelli, M. Le Tacon, M. Minola, S. Blanco-Canosa, C. Mazzoli, N. B. Brookes, G. M. De Luca, A. Frano, D. G. Hawthorn, F. He, T. Loew, M. M. Sala, D. C. Peets, M. Salluzzo, E. Schierle, R. Sutarto, G. A. Sawatzky, E. Weschke, B. Keimer, and L. Braicovich, Long-range incommensurate charge fluctuations in (Y, Nd)$Ba_2Cu_3O_{6+x}$, Science **337**, 821 (2012)

[13] R. Comin, R. Sutarto, F. He, E. H. da Silva Neto, L. Chauviere, A. Fraño, R. Liang, W. N. Hardy, D. A. Bonn, Y. Yoshida, H. Eisaki, A. J. Achkar, D. G. Hawthorn, B. Keimer, G. A. Sawatzky, and A. Damascelli, Symmetry of charge order in cuprates, Nat. Mater. **14**, 796 (2015).

[14] Y. X. Wang and A. V. Chubukov, Enhancement of superconductivity at the onset of charge-density-wave order in a metal, Phys. Rev. B **92**, 125108 (2015).

[15] H. Freire, V. S. de Carvalho, and C. Pépin, Renormalization group analysis of the pair-density-wave and charge order within the fermionic hot-spot model for cuprate superconductors, Phys. Rev. B **92**, 045132 (2015).

[16] M. Rotter, M. Tegel, and D. Johrendt, Superconductivity at 38 K in the Iron Arsenide $(Ba_{1-x}K_x)Fe_2As_2$, Phys. Rev. Lett. **101**, 107006 (2008).

[17] M. Yi, D. Lu, J. Chu, J. G. Analytis, A. P. Sorini, A. F. Kemper, B. Moritz, S. Mo, R. G. Moore, M. Hashimoto, W. Lee, Z. Hussain, T. P. Devereaux, I. R. Fisher, and Z. X. Shen, Symmetry-breaking orbital anisotropy observed for detwinned $Ba(Fe_{1-x}Co_x)_2As_2$ above the spin density wave transition, Proc. Natl. Acad. Sci. (USA) **108**, 6878 (2011).

[18] M. G. Kim, R. M. Fernandes, A. Kreyssig, J. W. Kim, A. Thaler, S. L. Bud'ko, P. C. Canfield, R. J. McQueeney, J. Schmalian, and A. I. Goldman, Character of the structural and magnetic phase transitions in the parent and electron-doped $BaFe_2As_2$ compounds, Phys. Rev. B **83**, 134522 (2011).

[19] J.-H. Chu, H.-H. Kuo, J. G. Analytis, and I. R. Fisher, Divergent nematic susceptibility in an iron arsenide superconductor, Science **337**, 710 (2012).

[20] R. M. Fernandes, A. V. Chubukov, and J. Schmalian, What drives nematic order in iron-based superconductors? Nat. Phys. **10**, 97 (2014).

[21] F. Ronning, N. Kurita, E. D. Bauer, B. L. Scott, T. Park, T. Klimczuk, R. Movshovich, and J. D. Thompson, The first order phase transition and superconductivity in $BaNi_2As_2$ single crystals, J. Phys.: Condens. Matter **20**, 342203 (2008).

[22] K. Kudo, Y. Nishikubo, and M. Nohara, Coexistence of superconductivity and charge density wave in $SrPt_2As_2$, J. Phys. Soc. Jpn. **79**, 123710 (2010).

[23] M. Imai, S. Emura, M. Nishio, Y. Matsushita, S. Ibuka, N. Eguchi, F. Ishikawa, Y. Yamada, T. Muranaka, and J. Akimitsu, Superconductivity in 122 antimonide $SrPt_2Sb_2$, Supercond. Sci. Technol. **26**, 075001 (2013).

[24] A. F. Fang, T. Dong, H. P. Wang, Z. G. Chen, B. Cheng, Y. G. Shi, P. Zheng, G. Xu, L. Wang, J. Q. Li, and N. L. Wang, Single-crystal growth and optical conductivity of $SrPt_2As_2$ superconductors, Phys. Rev. B **85**, 184520 (2012).

[25] A. Imre, A. Hellmann, G. Wenski, J. Graf, D. Johrendt, and A. Mewis, Modulated crystal structures and phase transitions—The compounds $SrPt_2As_2$ and $EuPt_2As_2$, Z. Anorg. Allg. Chem. **633**, 2037 (2007).

[26] L. Wang, Z. Wang, H.-L. Shi, Z. Chen, F.-K. Chiang, H.-F. Tian, H.-X. Yang, A.-F. Fang, N.-L. Wang, and J.-Q. Li,

Two-coupled structural modulations in charge-density-wave state of $SrPt_2As_2$ superconductor, Chin. Phys. B **23**, 086103 (2014).

[27] S. Kawasaki, Y. Tani, T. Mabuchi, K. Kudo, Y. Nishikubo, D. Mitsuoka, M. Nohara, and G. Q. Zheng, Coexistence of multiple charge-density waves and superconductivity in $SrPt_2As_2$ revealed by ^{75}As-NMR/NQR and ^{195}Pt-NMR, Phys. Rev. B **91**, 060510(R) (2015).

[28] W. B. Jiang, C. Y. Guo, Z. F. Weng, Y. F. Wang, Y. H. Chen, Y. Chen, G. M. Pang, T. Shang, X. Lu, and H. Q. Yuan, Superconductivity and structural distortion in $BaPt_2As_2$, J. Phys.: Condens. Matter **27**, 022202 (2015).

[29] N. R. Werthamer, E. Helfand, and P. C. Hohenberg, Temperature and purity dependence of the superconducting critical field, H_{c2}. III. Electron spin and spin-orbit effects, Phys. Rev. **147**, 295 (1965).

[30] K. Murata, H. Yoshino, H. O. Yadav, Y. Honda, and N. Shirakawa, Pt resistor thermometry and pressure calibration in a clamped pressure cell with the medium, Daphne 7373, Rev. Sci. Instrum. **68**, 2490 (1997).

[31] F. Ronning, E. D. Bauer, T. Park, S.-H. Baek, H. Sakai, and J. D. Thompson, Superconductivity and the effects of pressure and structure in single-crystalline $SrNi_2P_2$, Phys. Rev. B **79**, 134507 (2009).